Analytic solutions to the Boltzmann equation for electron transport in silicon

L. R. Logan, H. H. K. Tang, and G. R. Srinivasan
Theoretical Modeling Department, IBM East Fishkill Laboratory, Hopewell Junction, New York 12533
(Received 12 October 1990)

Using a time-dependent Boltzmann-equation formalism, we have developed a model for electron transport in a semiconductor material subject to external electric fields. As an illustration of this work, we have investigated the electron-transport properties in silicon. We have included both electron-electron and intervalley electron-phonon scattering mechanisms modeled in the relaxation-time approximation. We have calculated the low-order moments of the Boltzmann equation as a function of time and as a function of the applied electric-field strength. Reasonable agreement is found between our model and previous Monte Carlo simulations [Phys. Rev. B **38**, 9721 (1988)].

I. INTRODUCTION

Semiclassical Boltzmann transport equations (BTE's), implemented with appropriate collision terms, provide a general theoretical framework for a variety of condensed-matter problems. Time-dependent solutions of these equations contain information on the equilibrium and nonequilibrium properties of many-body systems. For example, the properties of condensed plasmas,[1] the evolution of atomic nuclei under extreme conditions,[2] and the electronic transport in solids[3] can all be conveniently studied by means of Boltzmann-equation transport theories.

In the case of modeling modern semiconductor devices, the BTE would have been an ideal approach, except for a number of conceptual and technical difficulties. The collision term associated with the carrier-carrier scatterings, even in the lowest-order theory (say, Born approximation with a screened Coulomb potential[4]), already makes the BTE highly nonlinear. Furthermore, the band structure of the semiconductor material and the electron-phonon coupling introduce additional complex collision terms which are absent in the theory of simple plasmas.

There have been several analytical and numerical methods for approximating the solution of the BTE that have been reported in the literature. The two most popular analytical techniques for time-independent solutions involve the following. (i) One assumes a certain analytical form for the electron distribution that depends upon some parameters which are then determined from the BTE (e.g., see Ref. 3). (ii) The distribution function is expanded in a series of Legendre polynomials to yield an infinite set of coupled equations for the expansion coefficients (e.g., see Ref. 5). One of the more widely used numerical techniques for the solution of the BTE is through solving the equivalent integral equation by iteration (e.g., see Ref. 6). The most popular numerical methods used to solve the BTE are Monte Carlo simulations (e.g., Ref. 7). Although these are very powerful techniques they are not without limitations. The large amount of numerical simulation often obscures the underlying physical picture. These numerical techniques leave the fundamental questions of the dominant scattering mechanisms unresolved. In particular, phenomenological scattering matrices must be used in Monte Carlo calculations.[7–9]

A complementary approach involves the use of macroscopic, hydrodynamic-type transport equations (e.g., see Ref. 10), derived from the BTE. Since the quantities of physical interest correspond to low-order moments of the electron distribution (typically zeroth, first, and second, which represent densities in charge, momentum and energy, respectively) there are obvious advantages in formulating models that focus on only a finite number of moments. Standard hydrodynamical models, however, suffer from several major shortcomings. First, the truncation of an infinite hierarchy of moment equations makes it necessary to invoke *ad hoc* assumptions. For example, the energy-flux equation derived from the second moment of the BTE contains a term involving third-order moments. Hence, in the conventional hydrodynamic model one must introduce a thermal conductivity term which relates the second- and third-order moments. This assumption then imposes a closure on the moment equation hierarchy, but it is done without much theoretical justification. Second, in the context of the electronic transport in semiconductors, it is necessary to use a set of phenomenological transport coefficients such as the macroscopic momentum and energy relaxation times and carrier mobilities to simulate realistic transport properties in semiconductor material. How these important macroscopic parameters are related to the underlying microscopic scattering mechanisms is unclear. Third, the crucial assumption inherent to the conventional hydrodynamic approach is that the system is locally equilibrated (i.e., the distribution is, at each point in phase space, a Maxwellian distribution characterized by local densities in energy, momentum, and charge) so that the temperature is treated as a scalar quantity. With modern miniaturized devices under strong electric fields it is unlikely that this condition will be satisfied. Indeed, the work of Wingreen, Stanton, and Wilkens[11] suggests that with a finite electron-electron scattering rate, an anisotropy in the distribution function occurs even at modest electric-

 ©1991 The American Physical Society

field strengths.

In this work, we examine some of these theoretical issues which are important for future development of device simulators. In Sec. II, we formulate a BTE incorporating an external electric field and with collision terms modeled in the relaxation-time approximation. These collision terms represent both electron-electron and intervalley electron-phonon scatterings. The solution of this BTE is obtained through the use of an exact-integral representation. To the extent that this simplified BTE already incorporates most of the important scattering mechanisms, many of the properties of the system can now be calculated readily. In Sec. III, we show by numerical examples that the solutions of our BTE agree well with large-scale Monte Carlo simulations. We compute the lower-order moments of the BTE (i.e., drift velocity and temperature tensor) as a function of time and external electric-field strength. The explicit time-dependent solutions provide insight into the transient behavior of the system and its modeling using the hydrodynamic approach. Furthermore, transient analysis is difficult using a Monte Carlo technique. The solutions of the BTE presented here may be useful in future modeling efforts involving time-dependent phenomena. In Sec. IV, we summarize our findings and discuss the future prospects of extending this work for applications involving realistic devices.

II. THEORY

We are presenting a model for electron transport subject to external electric fields in bulk semiconductor material. Our focus in the present work is transport properties in silicon and results pertaining to that element are given in Sec. III. Collisional effects are modeled using the relaxation-time approximation. We assume that the electron-electron interaction is elastic so that its effect is to redistribute energy within the distribution while maintaining conservation of total charge, momentum, and energy. The scattering rate for this interaction, $\tau_{e\text{-}e}^{-1}$, is taken to be constant. To account for electron-phonon interactions, we include both equivalent and nonequivalent intervalley scattering. In silicon these correspond to X-to-X and X-to-L intervalley transitions. The phonon scatterings are dissipative in energy but conserve total charge. The scattering rates for these mechanisms are explicitly functions of the carrier energy. Our model does not include spatial correlation effects (e.g., effects due to temperature gradients) since we are taking the electron distribution function $f(\mathbf{p},t)$ to be uniform in space. Using the above prescription, the Boltzmann equation that we are solving is written as

$$\left[\frac{\partial}{\partial t}-e\mathbf{E}\cdot\nabla_p\right]f(\mathbf{p},t)=-\frac{f(\mathbf{p},t)-f_1(\mathbf{p},t)}{\tau_{e\text{-}e}}-\sum_{i=2}^{11}\frac{f(\mathbf{p},t)-f_i(\mathbf{p},t)}{\tau_{e\text{-ph}}^{(i)}(\mathbf{p})}\ , \qquad (2.1)$$

where e is the electronic charge and $\mathbf{E}$ is a constant applied electric field. The functions $f_1(\mathbf{p},t)$ and $f_i(\mathbf{p},t)$ are the distribution functions towards which $f(\mathbf{p},t)$ tends to relax due to the scattering interactions. These are described below. For X-to-X intervalley scattering there are six phonon branches, three f (scattering to adjacent valleys), and three g (scattering to opposite valleys). In the case of X-to-L intervalley scattering there are four phonon terms. Therefore, there is total of ten electron-phonon scattering terms appearing on the right-hand side of the BTE (2.1).

Let us first discuss the situation in which only the elastic electron-electron scattering is considered. In this case, due to Boltzmann's H theorem, we would expect that at asymptotically large time the electron distribution function would approach a Gaussian. Motivated by this we write the relaxation function for the electron-electron term in (2.1) as

$$f_1(\mathbf{p},t)=\frac{\rho_0}{[2\pi m^*T(t)]^{3/2}}\exp\left[\frac{-[\mathbf{p}-\langle\mathbf{p}(t)\rangle]^2}{2m^*T(t)}\right]\ , \qquad (2.2)$$

where m^* is an effective mass and $T(t)$ is the electron temperature at time t. Here, and in what follows, we have set Boltzmann's constant k_B equal to one. The function $f_1(\mathbf{p},t)$ represents the electron distribution under conditions of local equilibrium at temperature $T(t)$. The quantities in the angular brackets are averages defined as follows: For any quantity $\chi(\mathbf{p},t)$ we define the average $\langle\chi(\mathbf{p},t)\rangle$ to be given by

$$\langle\chi(\mathbf{p},t)\rangle=\frac{1}{\rho_0}\int d^3p\,\chi(\mathbf{p},t)f(\mathbf{p},t)\ , \qquad (2.3)$$

where ρ_0 is the number density. The temperature $T(t)$ is given by

$$T(t)=\frac{1}{3m^*}[\langle p(t)^2\rangle-\langle\mathbf{p}(t)\rangle^2]\ . \qquad (2.4)$$

The relaxation distribution $f_1(\mathbf{p},t)$ is a functional of $f(\mathbf{p},t)$ and therefore the BTE give by (2.1) is highly nonlinear.

The function $f_i(\mathbf{p},t)$ represents the equilibrium distribution that the ith electron-phonon interaction drives $f(\mathbf{p},t)$ towards. Since there is no analogous counterpart to the H theorem for the case of inelastic interactions we do not have a rigorous prescription for the relaxation function, $f_i(\mathbf{p}t)$. We have modeled it based on analogy with the electron-electron scattering, in which the relaxation function is Gaussian as discussed above. Making the assumption that the electron-phonon interaction may be treated in this way, we propose a relaxation function of the type

$$f_i(\mathbf{p},t)=\frac{N(t)}{(2\pi m^*T_l)^{3/2}}e^{-p^2/2m^*T_l}\quad\text{for } i\neq 1\ , \qquad (2.5)$$

where T_l is the lattice temperature and $N(t)$ is a normalization function that we describe below.

In the case where one considers only elastic electron-electron scattering the solution to the BTE must conserve particle number, momentum, and energy. If we specify an initial distribution function having the same normalization as the distribution $f_1(\mathbf{p},t)$ then the solution at later times preserves all of the required conservation properties. When the inelastic electron-phonon scattering is included we no longer have conservation of momentum or energy although the particle number should remain constant. This requirement leads to the following prescription for the normalization factor $N(t)$:

$$N(t)=\int d^3p \sum_{i=2}^{11} \frac{f(\mathbf{p},t)}{\tau_{e\text{-ph}}^{(i)}(\mathbf{p})}\left[\sum_{i=2}^{11}\int d^3p \frac{(2\pi m^* T_l)^{-3/2} e^{-p^2/2m^* T_l}}{\tau_{e\text{-ph}}^{(i)}(\mathbf{p})}\right]^{-1} . \tag{2.6}$$

With this definition for $N(t)$ we are assured that

$$\int d^3p\, f(\mathbf{p},t)=\rho_0 \quad \text{for all } t , \tag{2.7}$$

where ρ_0 is the number density.

In our model we treat the BTE (2.1) as an initial-value problem. Given the initial distribution function $f_0(\mathbf{p})$ at time zero, the general solution at some later time t takes the form

$$\begin{aligned} f(\mathbf{p},t)=&f_0(\mathbf{p}+\mathbf{F}t)\exp\left[-\int_0^t dt' \frac{1}{\tau(\mathbf{p}+\mathbf{F}(t-t'))}\right] \\ &+\exp\left[-\int_0^t dt' \frac{1}{\tau(\mathbf{p}+\mathbf{F}(t-t'))}\right]\int_0^t dt' \exp\left[\int_0^{t'} dt'' \frac{1}{\tau(\mathbf{p}+\mathbf{F}(t-t''))}\right] \\ &\times\left[\frac{f_1(\mathbf{p}+\mathbf{F}(t-t'))}{\tau_{e\text{-}e}}+\sum_{i=2}^{11}\frac{f_i(\mathbf{p}+\mathbf{F}(t-t'))}{\tau_{e\text{-ph}}^{(i)}(\mathbf{p}+\mathbf{F}(t-t'))}\right] , \end{aligned} \tag{2.8}$$

where $\mathbf{F}=|e|\mathbf{E}$ is the applied electrical force. The overall effective scattering rate $\tau(\mathbf{p})$ is given by

$$\frac{1}{\tau(\mathbf{p})}=\sum_{i=2}^{11}\frac{1}{\tau_{e\text{-ph}}^{(i)}(\mathbf{p})}+\frac{1}{\tau_{e\text{-}e}} . \tag{2.9}$$

Note that (2.8) is an implicit equation for $f(\mathbf{p},t)$ due to the presence of the functions $f_i(\mathbf{p},t)$ on the right-hand side. Thus the original problem of solving the BTE (1) is equivalent to solving the highly nonlinear integral equation (2.8). From the latter we can calculate moments of the electron distribution function which have the form

$$\langle p_i^n(t)p_j^m(t)\rangle=\frac{1}{\rho_0}\int d^3p\, p_i^n p_j^m f(\mathbf{p},t) \qquad (i,j)=(x,y,z) . \tag{2.10}$$

We are particularly interested in examining $\langle \mathbf{p}(t)\rangle$, $\langle p^2(t)\rangle$, and the temperature $T(t)$, which are the most important from the device design point of view. It is also instructive to evaluate the moments $\langle p_i(t)p_j(t)\rangle$ for $i\neq j$ which are a measure of the degree to which the system is off equilibrium. The latter are important since they give us information on the limits of validity of conventional hydrodynamic modeling.

In the present model we evaluate the various intervalley scattering rates $\tau_{ij}(\mathbf{p})$ as follows: we take the transition probability for scattering from a state $\mathbf{p}'$ in valley i to a state $\mathbf{p}$ in valley j via an interaction with a phonon having a frequency ω_{ij} to be given by[7]

$$W_{ij}(\mathbf{p},\mathbf{p}')=z_j\frac{D^2}{8\pi^2\rho\omega_{ij}}\begin{Bmatrix} n_0+1 \\ n_0 \end{Bmatrix}\delta(\varepsilon(\mathbf{p})-\varepsilon(\mathbf{p}')-\Delta_{ij}\pm\hbar\omega_{ij}) . \tag{2.11}$$

where D is a coupling constant, ρ is the density of the material, $\varepsilon(\mathbf{p})$ is the carrier energy, $z_j^{2/3}m_d^*$ is the density of states effective mass for the set of equivalent final valleys indexed by j, and Δ_{ij} is the energy difference between the minima of valley j and valley i. The functional form $\varepsilon(\mathbf{p})$ is determined by the assumed band-structure model. We define the scattering rate τ_{ij}^{-1} to be the intrinsic lifetime of state $\mathbf{p}$, viz.,

$$\frac{1}{\tau_{ij}(\mathbf{p})}=\int d^3p' W_{ij}(\mathbf{p},\mathbf{p}') . \tag{2.12}$$

In the case where the band structure is taken to be spherical parabolic, it is easy to show that the total scattering rate $\tau_{ij}^{-1}(\mathbf{p})$ is given by

$$\begin{aligned}\frac{1}{\tau_{ij}(\mathbf{p})}=&z_j\frac{m_d^{*3/2}D^2}{\sqrt{2}\pi\rho\hbar^3\omega_{ij}} \\ &\times[n_0\sqrt{\varepsilon(\mathbf{p})-\Delta_{ij}+\hbar\omega_{ij}} \\ &+(n_0+1)\sqrt{\varepsilon(\mathbf{p})-\Delta_{ij}-\hbar\omega_{ij}}] ,\end{aligned} \tag{2.13}$$

where

$$n_0=(e^{\hbar\omega_{ij}/T_l}-1)^{-1} \tag{2.14}$$

is the phonon occupation number. We assume that the phonon distribution is in equilibrium with the lattice so that n_0 has the Bose-Einstein form as above.

As far as the choice of scattering mechanisms is concerned, we comment that the choice of including only electron-electron and intervalley (electron-phonon) scattering is not due to any restriction of the model. We

can include any other type of scattering that can be modeled in a relaxation-time approximation. Of course, the corresponding scattering rates can depend on momentum in an arbitrary manner. Since in the present study we have not included impact ionization effects we would be uncertain of any results obtained using a field larger than ~100 kV/cm. In fact, the use of a relaxation-time approximation is itself questionable at such high fields.

We have also investigated the effect of including nonparabolicity in the band structure by writing the energy–wave vector relationship in the form

$$\varepsilon(1+\alpha\varepsilon)=\frac{\hbar^2k^2}{2m^*} . \tag{2.15}$$

In the above α is the nonparabolicity parameter which for silicon is 0.5 eV^{-1}. We have found that including this gives rise to only a very small effect on the results (only a few percent). Since we cannot expect high-precision accuracy in the present study we have chosen to use a parabolic band-structure model in favor of computational simplicity.

The results from the present model can be used to estimate the macroscopic momentum and energy relaxation times that are used in the hydrodynamical model. We denote the latter by τ_p and τ_w, respectively. The relations

$$\tau_p=\frac{m^*v_{\text{st}}}{e|\mathbf{E}|} \tag{2.16}$$

and

$$\tau_w=\frac{\varepsilon-\varepsilon_0}{ev_{\text{st}}|\mathbf{E}|} \tag{2.17}$$

provide a mapping between the two models. In the above, v_{st} is the steady-state drift velocity, and ε_0 is the equilibrium electron energy $\frac{3}{2}T_l$. We find, for example, that for an applied field of 50 kV/cm at a lattice temperature of 300 K the momentum relaxation time is 1.3×10^{-13} sec and the corresponding energy relaxation time is 1.1×10^{-13} sec. The latter may be compared with the value of 4.0×10^{-13} sec as determined from a Monte Carlo study.[12] Interestingly, recent hydrodynamic device simulation studies have found that the energy relaxation time extracted from Monte Carlo simulations could not be used to reproduce experimental results on bulk currents versus gate and drain voltages.[13] The required value of τ_w was about four times smaller than the value determined from the Monte Carlo simulation, which is close to the value determined in this work.

III. RESULTS AND DISCUSSION

In the present case we are investigating the transport properties of electrons in silicon. Since the method is completely general, we could equally well have chosen another semiconductor material for study. Silicon is, however, a convenient choice since there is a wealth of experimental and theoretical information available on electron-transport properties (e.g., see Refs. 12 and 14).

For simplicity we choose the initial distribution to be a Gaussian centered at an initial momentum $\mathbf{p}_0$ and with a width determined by an initial temperature T_0. Hence $f_0(\mathbf{p})$ is given by

$$f_0(\mathbf{p})=\frac{1}{(2\pi m^*T_0)^{3/2}}\exp\left[\frac{-(\mathbf{p}-\mathbf{p}_0)^2}{2m^*T_0}\right] . \tag{3.1}$$

The values that one takes for $\mathbf{p}_0$ and T_0 are a matter of choice. We have taken T_0 to be 300 K and the initial momentum $\mathbf{p}_0$ to be zero. For the effective mass we have used a value of $1.09m_0$ (m_0 is the free-electron mass) which represents the density of states effective for the X valleys in silicon. In the above $f_0(\mathbf{p})$ is normalized so that $\rho_0=1$ [see Eq. (2.7)].

The first conduction band in silicon has six equivalent minima along the X symmetry directions. The second conduction band has minima that are located along the eight L symmetry directions. The energy of the latter are about 1-eV higher than the minima in the X valleys. Hence the Δ_{ij} terms in Eq. (2.13) are 0 and 1 eV for X-to-X and X-to-L intervalley scattering, respectively. To complete the determination of the intervalley scattering rates we must specify the electron-phonon coupling constants D and phonon energies $\hbar\omega_{ij}$. For the X-to-X intervalley transitions we have used the coupling constants and phonon energies given by Fischetti and Laux[8] and for the X-to-L transitions the coupling constants and phonon energies given by Tang and Hess[9] have been used. There is clearly no definitive choice in this matter and we have used these values simply to illustrate the method in a consistent way. The values for these constants are summarized in Table I and more discussion on this issue is given below. The total electron-phonon scattering rate for intervalley transitions is shown in Fig. 1 as a function of the carrier energy. In this figure the dashed and dotted curves indicate the absorption and

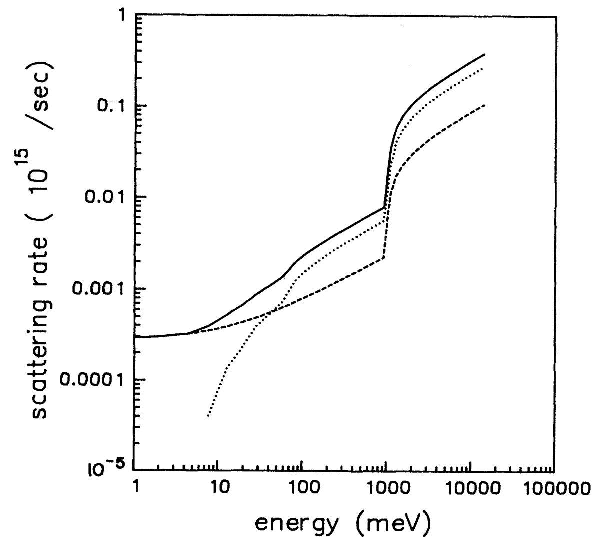

FIG. 1. Intervalley electron-phonon scattering rates in silicon at 300 K. The electron-phonon coupling constants and phonon energies used are those from Refs. 8 and 9 for X-to-X and X-to-L transitions, respectively. The dashed curve shows the total absorption rate whereas the dotted curve shows the total emission rate. The total scattering rate is the sum of these two and is shown by the solid curve.

TABLE I. Electron-phonon coupling constants and corresponding phonon energies for electron intervalley scattering in silicon. The coupling constants D are in units of 10^8 eV/cm and the phonon energies $\hbar\omega_{ij}$ are in meV.

	X-to-X transitions			
	Canali *et al.* (Ref. 14)		Fischetti and Laux (Ref. 8)	
Type	D	$\hbar\omega_{ij}$	D	$\hbar\omega_{ij}$
f_1	0.15	18.1	0.3	14.7
f_2	3.4	43.1	0.3	7.2
f_3	4.0	54.3	1.75	62.0
g_1	0.5	12.1	1.18	44.3
g_2	0.8	18.1	1.18	22.1
g_3	3.0	60.3	1.75	62.0
	X-to-L transitions			
	Sano *et al.* (Ref. 16)		Tang and Hess (Ref. 9)	
	D	$\hbar\omega_{ij}$	D	$\hbar\omega_{ij}$
	4.0	57.9	2.5	57.9
	4.0	54.6	2.5	54.6
	4.0	41.4	2.5	41.4
	4.0	17.0	2.5	17.0

emission rates and their sum, the total scattering rate, is shown by the solid curve. The form of these curves is easily understood from the scattering mechanism incorporated in the present model. The emission rate for the ith interaction must obviously be zero when the carrier energy is less than the corresponding phonon energy. Hence the emission curve in Fig. 1 drops to zero at 7.2 meV (the minimum phonon energy that gives rise to an intervalley transition). The threshold energies for the remaining X-to-X transitions are all within about a factor of 8 of this value. Hence we see the total scattering rate rise appreciably in this energy region. The next threshold occurs at about 1 eV where the onset of the X-to-L transitions occur. Since the coupling constants and overall density-of-states effective mass for the L valleys are quite large, the X-to-L transitions contribute strongly to the total scattering rate. In the present model, however, we are confining our attention to external fields less than about 100 keV/cm and therefore the X-to-L transitions play a minor role in determining the transport properties in comparison to the X-to-X transitions. Hence the electron-phonon interaction serves to dissipate the overall e carriers' energy when it is in excess of the lattice thermal energy. In the results that follow we shall see that equilibrium conditions are obtained through a balancing of effects due to the accelerating electric field and the dissipative electron-phonon interaction.

In Fig. 2 we show the calculated distribution function $F(\varepsilon,t)$ as a function of energy ε for three different times as indicated. We define $F(\varepsilon,t)$ as follows:

$$F(\varepsilon,t)=\int f(p,\theta,t)\delta(p^2/(2m^*)-\varepsilon)d^3p$$
$$=2\pi m^*\int f(\sqrt{2m^*\varepsilon},t)\sqrt{2m^*\varepsilon}\,\sin\theta\, d\theta\ . \qquad (3.2)$$

The lattice temperature in all three cases is 300 K and the applied electric-field strength is 100 kV/cm. The initial distribution is a Gaussian characterized by Eq. (3.1). Due to the accelerating effects of the external electric field the distribution at later times is shifted toward higher energies. The distributions shown in the figure correspond to the transient response at 0.1 psec and steady-state conditions at 0.5 psec. We comment finally that information on the shape of the distribution functions, such as that shown in Fig. 2, is generally not obtainable from theories which describe only the moments

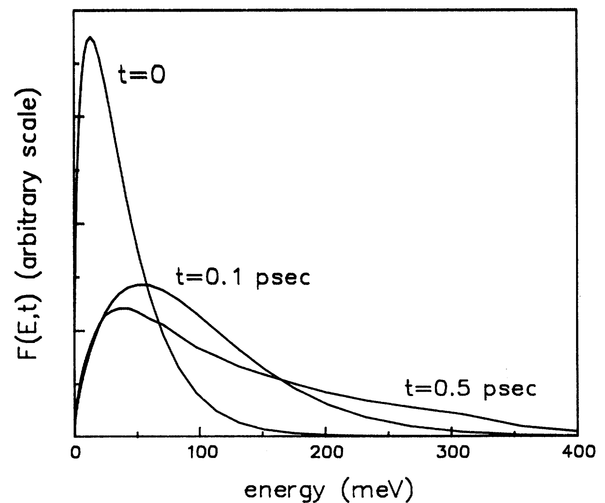

FIG. 2. The energy-distribution function at various times for electrons in silicon at 300 K subject to an external field of 100 kV/cm. The energy-distribution function is defined by Eq. (3.2) in the text. The indicated times correspond to the following situations: (i) at $t=0$ the distribution is in its initial state given by Eq. (3.1) with $T_0=300$ K, (ii) $t=0.1$ psec shows the distribution during the transient response of the system, and (iii) $t=0.5$ psec shows the distribution under steady-state conditions.

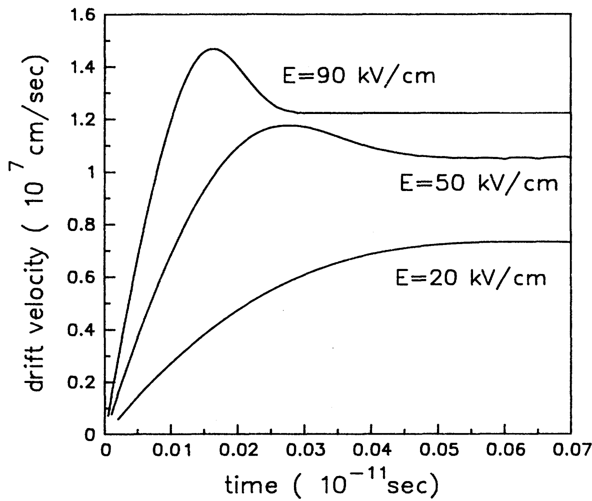

FIG. 3. Electron-drift velocity in silicon at 300 K as a function of time for selected values of the electric field. Overshoot effects clearly become more pronounced as field strength is increased. The transient time scales are consistent with those calculated by Nougier *et al.* (Ref. 15) for electric fields in the same range.

of $f(\mathbf{p},t)$. In this regard, models of this type which explicitly calculate the distribution function are physically more insightful.

Figure 3 shows results for electron drift velocity in silicon at 300 K as a function of time for several values of the external electric field. Since in these calculations we have treated all X valleys equivalently the results would correspond to the situation where the field is in the $\langle 111 \rangle$ direction. Regardless of this, experimental results[14] show only a very small difference between results of this type obtained with electric fields along the $\langle 111 \rangle$ and $\langle 100 \rangle$ directions. All of the results show that the electron drift velocity saturates after some transient time which depends on the electric-field strength. These transient times are consistent with those calculated earlier by Nougier *et al.*[15] The curves that correspond to 50 and 90 keV/cm show some velocity overshoot prior to becoming steady state. This feature is also found in the work of Nougier *et al.* although the present model predicts a smaller degree of this effect. Both models, however, predict the disappearance of the overshoot as the electric field is decreased.

The magnitude of the steady-state velocity versus applied field strength is plotted in Fig. 4. Shown for comparison are similar results obtained from a Monte Carlo approach.[8] Despite the simplicity of our model there is a reasonable correspondence between the two sets of results. It is significant to point out that we have used the values of the electron-phonon coupling constants and phonon energies given in Refs. 8 and 9 for X-to-X and X-to-L intervalley transitions, respectively) without adjustments. We could have undoubtedly achieved a much better agreement if adjustments to these constants were made. Indeed, as very little is known about the values for these coupling constants, one chosen set is meaningful only within the model from which they are obtained. In comparison to various sets of constants we see that there is generally poor agreement on their precise values (see Table I). For a given model these sets are chosen to render agreement with the experimental velocity versus

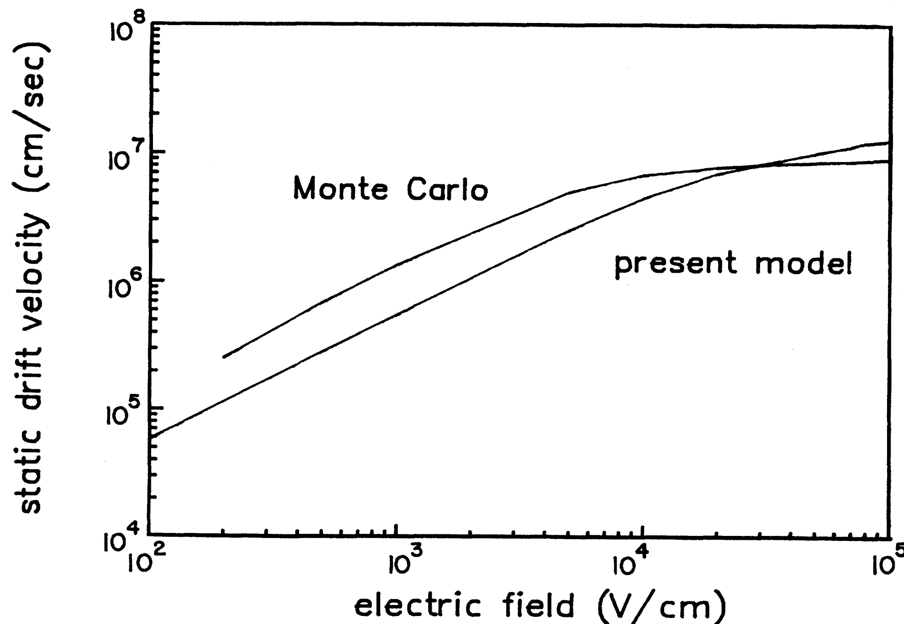

FIG. 4. Static drift velocity as a function of electric-field strength for electrons in Si at 300 K. The Monte Carlo results are taken from Ref. 8.

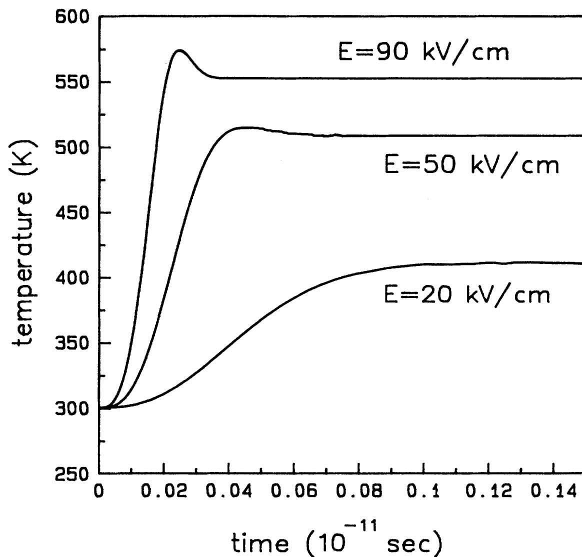

FIG. 5. Electron temperature as a function of time for selected values of electric-field strength in silicon. The temperatures of the initial electron distribution and the lattice were set to 300 K.

field curves.[14] The fact that our velocity versus field curve agrees reasonably well with the Monte Carlo results (and hence with experimental data) is quite remarkable given that we had no adjustable parameters.

In Fig. 5 we show calculated values of the electron temperature $T(t)$ as a function of time. As in Fig. 3 we see that the temperature reaches a steady-state value after some characteristic transient time. We note that the transient rise in temperature is less rapid than that corresponding to velocity as in Fig. 3. Similar to the velocity curves in Fig. 2, there is an overshoot effect but to a lesser degree in this case.

The steady-state versus electric-field strength is shown in Fig. 6. Similar to previous studies[8,9] the energy is nearly constant up to about 10 kV/cm. We find generally that the energy values above 10 kV/cm are smaller than those reported previously.[8,9] It is important to note, however, that a comparison between the steady-state energies as obtained from the aforementioned references are themselves rather different above roughly 50 kV/cm. As mentioned above, the parameters for these studies were chosen to give results matching the experimental velocity versus field curves (i.e., the first moment of BTE) but it is not guaranteed that all such studies will agree on higher-order moments such as energy. It is therefore not surprising that the present model gives results different from the Monte Carlo studies. Of course, there are no experiments which measure the carrier energy as a function of electric-field strength so it is unclear which set of results is closer to reality.

In the case where one develops a theory involving only the zeroth-, first-, and second-order moments of the BTE one encounters a temperature tensor with components

$$T_{ij}(t)=\frac{1}{3m^{*}\rho_0}\int(p_i-\langle p_i\rangle)(p_j-\langle p_j\rangle)f(\mathbf{p},t)d^3p \tag{3.3a}$$

or equivalently,

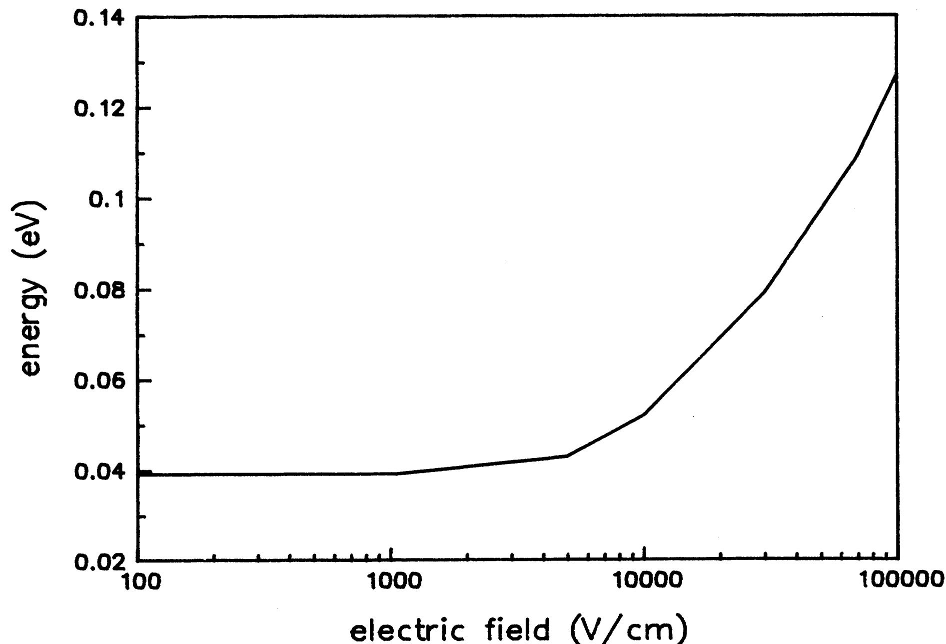

FIG. 6. Total electron energy as a function of applied electric-field strength for electrons in silicon at 300 K. The values in the low-field region tend towards the lattice thermal energy, $\frac{3}{2}k_B T_l$.

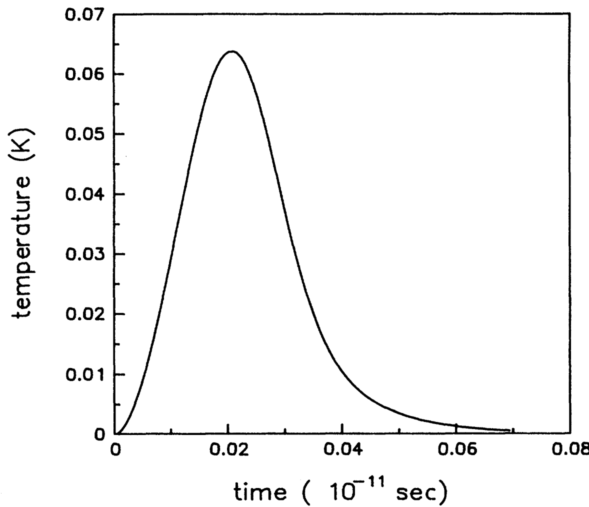

FIG. 7. Off-diagonal temperature tensor component T_{xz} for electrons in silicon at 300 K with an applied field of 70 kV/cm in the $\hat{\mathbf{z}}$ direction. The coordinates x and z define a two-dimensional coordinate system with components parallel and perpendicular to the electric field, respectively. The initial conditions were set arbitrarily to be $\mathbf{p}(t=0)=0.001e|\mathbf{E}|\tau_{e\text{-}e}\hat{\mathbf{x}}$ and $T_0=300$ K.

$$T_{ij}(t)=\frac{1}{3m^*}(\langle p_i p_j\rangle-\langle p_i\rangle\langle p_j\rangle) . \quad (3.3b)$$

In Fig. 7 we show a plot of $T_{xz}(t)$ versus time where the coordinates z and x are in the directions parallel and perpendicular to the external field, respectively. For the calculation of this quantity we have used a two-dimensional coordinate system for computational simplicity. In this case the initial distribution function is Gaussian with a very small drift term in the direction perpendicular to the field [$\mathbf{p}(t=0)=0.001e|\mathbf{E}|\tau_{e\text{-}e}\hat{\mathbf{x}}$]. Due to the Gaussian form of the initial distribution T_{xz} is identically zero at $t=0$. As the distribution reacts to the external field the original symmetry is lost and nonzero values of T_{xz} appear. Finally, after a certain amount of time the distribution reached equilibrium and the off-diagonal terms vanish. The time scale during which the T_{xz} is nonzero is of interest in the context of the hydrodynamical model as we now discuss. The conventional hydrodynamical model considers only the equilibrium case where $T_{ij}=0$ for $i\neq j$. The electron temperature is then a scalar given by $T=\frac{1}{3}(T_{xx}+T_{yy}+T_{zz})$. Therefore, an off-diagonal temperature tensor component with a long lifetime would imply that the distribution is not at local equilibrium during much of its transport and we would expect that including these off-diagonal components would be necessary in the hydrodynamical model. From Fig. 7, corresponding to an applied field of 70 kV/cm, we see that the T_{xz} is nonzero for about 0.6 psec and that this time scale is insensitive to the initial conditions. We caution the reader that the curve shown in Fig. 7 is presented only to illustrate the basic ideas. The magnitude of the off-diagonal term in this example cannot be used to make quantitative statements on the validity of hydrodynamics since we have chosen the initial transverse momentum in an arbitrary manner. We do, however, note that a typical time scale for nonzero T_{xz} can become appreciable. Hence, the tensorial nature of the temperature can become important in modern day applications where device sizes are in the submicron range with corresponding electric field in order of 100 kV/cm.

IV. CONCLUSIONS

We have presented a model for electron transport in bulk silicon in the presence of external electric fields. For the static velocity dependence of electric field we have found reasonable agreement with previous Monte Carlo studies.[8,9] We do find some quantitative differences in the results, but these are not unexpected since no parameter fitting is incorporated in the present work. As the present model explicitly calculates the distribution function it is much easier to calculate higher-order moments than using a Monte Carlo method. This issue may gain importance in the future since current research on generalized hydrodynamical models requires some knowledge of the third-order moments. It is well known that the Monte Carlo technique becomes less efficient as one attempts to calculate higher-order moments.

We have observed both equilibrium and nonequilibrium behavior of the electron distribution through the numerical examples presented in Sec. III. The time evolution of the distribution, in our model, is governed by the competing effects of energy loss and gain through the phonon interactions and external field, respectively. The BTE used in this study has been constructed explicitly with detailed electron-phonon scattering mechanisms. Insofar as the relaxation-time approximation is valid, and the physical model is complete, the calculated time evolution of the distribution function provides us with unique insight into the role of electron-phonon interactions in transport phenomena. The physical model in this case contains only electron-electron and intervalley electron-phonon scattering and we would expect that for intermediate-range electric fields, say $10^3<|\mathbf{E}|<10^5$ V/cm, the intervalley scattering interactions are dominant. Of course, for very low fields one would have to incorporate scattering from ionized impurities and for very high fields impact ionization would become important.

The issue of parameter selection remains unresolved at present. Indeed, no attempt has been made to address this issue here since it is essentially a separate theoretical topic. In order to illustrate the use of our model we have presented results using electron-phonon coupling constants that have been independently determined from previous investigations (as discussed in Sec. III), and these values may not be the most appropriate ones.

The extension of the present model to include impurity-scattering interactions is currently underway. This is especially important for the very low field transport ($|\mathbf{E}|<10^3$, say). The issue of spatial correlation effects, such as those that would exist in devices, is presently being addressed. For this further analytical

techniques are being developed to calculate a fully time- and space-dependent distribution function $f(\mathbf{p},\mathbf{r},t)$ in the presence of external electric fields. We expect that the present results together with the future work mentioned above will provide a physical foundation for the estimation of hydrodynamic model parameters.

We comment finally that the technique is reasonably efficient from a computational viewpoint. A typical run from time equal to zero to steady state takes roughly 40 min on an IBM RISC 6000 workstation, and for a given electric-field strength, a single run determines all of the quantities of interest.

ACKNOWLEDGMENTS

We are grateful to A. Gnudi, F. Odeh, and T.-W. Tang for helpful discussions.

[1]J. L. Delcroix, *Plasma Physics* (Wiley and Sons, New York, 1965).
[2]G. F. Bertsch and S. Das Gupta, Phys. Rep. **160**, 189 (1988).
[3]E. M. Conwell, *High Field Transport in Semiconductors* (Academic, New York, 1967).
[4]L. P. Kadanoff and G. Baym, *Quantum Statistical Mechanics* (Benjamin, New York, 1962).
[5]J. Yamashita and M. Watanabe, Prog. Theor. Phys. **12**, 443 (1954).
[6]H. D. Rees, J. Phys. Chem. Solids **30**, 643 (1969).
[7]C. Jacoboni and L. Reggiani, Rev. Mod. Phys. **55**, 645 (1983).
[8]Massimo V. Fischetti and Steven E. Laux, Phys. Rev. B **38**, 9721 (1988).
[9]J. Y. Tang and Karl Hess, J. Appl. Phys. **54**, 5139 (1983).
[10]M. Rudan and F. Odch, Int. J. Comput. Math. Electr. Electron. Eng. **5**, 149 (1986).
[11]Nee S. Wingreen, Christopher J. Stanton, and John W. Wilkins, Phys. Rev. Lett. **57**, 1084 (1986).
[12]C. Jacoboni, C. Canali, G. Ottaviani, and A. Algerigi-Quaranta, Solid State Electron. **20**, 77 (1977).
[13]G. Baccarani (private communication).
[14]C. Canali, C. Jacoboni, F. Nava, G. Ottaviani, and A. Alberigi-Quaranta, Phys. Rev. B **12**, 2265 (1975).
[15]J. P. Nougier, J. C. Vaissiere, D. Gasquet, J. Zimmerman, and E. Constant, J. Appl. Phys. **52**, 825 (1981).
[16]N. Sano, T. Takahiro, M. Tomizawa, and A. Yoshii, Phys. Rev. B **41**, 12 122 (1990).